International Journal of Environmental Science and Technology (2024) 21:6615–6636
https://doi.org/10.1007/s13762-024-05499-7

ORIGINAL PAPER

Comprehensive investigation of the durability and mechanical properties of eco-friendly geopolymer concrete (alkali-activated)

A. Esparham[1] · S. Rezaei[2]

Received: 4 July 2023 / Revised: 30 December 2023 / Accepted: 4 February 2024 / Published online: 4 March 2024

Abstract

Today, concrete is the most widely used building material. Cement production releases about 7% of carbon dioxide gas into the atmosphere and increases greenhouse gases, so it seems necessary to use an alternative to Portland cement. In recent years, geopolymers have been considered a suitable and environmentally friendly alternative to conventional Portland cement. Geopolymer concrete can be made from different sources of alumina silicate. The main goal of this experimental research is to improve the properties of physical resistance and durability of geopolymer concrete, such as carbonation, chloride ion penetration and water absorption, in order to produce sustainable materials and replace ordinary cement. It has been determined that with the concentration of the alkaline solution of 12 M and the curing temperature of 90 degrees Celsius, the properties of mechanical resistance, impact resistance (energy absorption) and durability of geopolymer concrete are improved. Also, the results show that if alkaline solutions are combined, the sample containing 80% NaOH and 20% KOH has better mechanical properties, durability and higher modulus of elasticity than other cases. Also, in terms of the correlation matrix of the modulus of elasticity (percentage of compliance with the common concrete regulations), the best results are related to the T-N80K20 mixing design with concentrations of 8 and 12 M and at curing temperature of 90 degrees Celsius with the CEB regulations, and at a curing temperature of 25 °C was obtained according to ACI 365 and ACI 318 regulations.

Keywords Geopolymer · Carbonation · Depth of chloride ions · Mechanical properties · Energy absorption · Sodium hydroxide · Potassium hydroxide · Common concrete regulations

Introduction

Concrete is the most widely used material in the construction industry, after water, due to its special characteristics such as formability, availability of raw materials, and cheapness. It is expected that the need to use concrete will increase in the future, and this means an increase in the demand for the production of Portland cement as the main material. But the production process of Portland cement has disadvantages. The production of Portland cement releases a large amount of carbon dioxide into the atmosphere, so that the production of 1 ton of Portland cement causes the production of approximately 1 ton of carbon dioxide. On the other hand, climate change is one of the most serious concerns due to the phenomenon of global warming. The main reason for warming is the global emission of greenhouse gases. Carbon dioxide gas, with the emission of 65%, has the largest role in global warming among greenhouse gases. One of the ways to reduce pollution caused by cement production is to use new materials with cement properties as a suitable substitute for common cements, which in addition to reducing the harmful effects of the environment, also reduces energy consumption. Geopolymers are one of the materials that can be used in concrete as an adhesive material, also the use of by-products and industrial waste as the primary source for the production of geopolymeric concrete (GPC) not only reduces the harmful effects on the environment, but also leads to waste management (Aliabdo et al. 2019; Alireza Esparham 2022a, b; Esparham and Ghalatian 2022; Esparham and Moradikhou 2021a).

Editorial responsibility: Q. Aguilar-Virgen.

✉ A. Esparham
alireza.esparham@ut.ac.ir

[1] Department of Environmental Engineering, University of Tehran, Tehran, Iran

[2] Department of Civil Engineering, University of Tehran, Tehran, Iran

The concept of geopolymer was first proposed by the French scientist Joseph Davidoit in 1978 (Esparham et al. 2021). Geopolymers are inorganic polymers whose chemical composition is similar to zeolite materials, but unlike zeolites, their microscopic structure is amorphous. Replacing clinker with geopolymers as a bonding material may be a suitable method to reduce the use of clinker in cement and thus reduce the harmful environmental effects caused by it and the construction of GPC. GPC is concrete that uses alumina silicate materials rich in silicon (Si) and aluminum (Al) and alkaline solution as binder. Compared to concrete made from ordinary cement, this active alkali concrete has several advantages, including low production energy and much less environmental pollution due to the absence of clinker (Alireza Esparham 2022a, b; Esparham et al. 2021). Geopolymers are a suitable alternative to cement in concrete because on the one hand geopolymers are cheaper than traditional cements and organic polymers and on the other hand they are abundant. In addition, the temperature required for their production is much lower than traditional cement, which reduces the production and emission of CO2 (up to 80% reduction). Geopolymer materials are produced by activating aluminosilicate materials with alkaline solutions of silicate and alkali hydroxide and processing in the ambient temperature range up to 120 degrees Celsius. Depending on the curing temperature, geopolymers can have an amorphous to semicrystalline structure in nanodimensions (Esparham et al. 2023). Of course, this type of concrete has weaknesses and problems, including the lack of valid criteria for design, proper performance, quick setting and the lack of comprehensive examination of permeability, durability and physical properties, especially at ambient temperature. Matching the results of the properties of this type of concrete with common regulations is one of the other things that have not been investigated in other studies (Chau-Khun et al. 2018; Kumar et al. 2018). The effect of molarity, the ratio of silicate to hydroxide, the amount of glue and the amount of superplasticizer and the effect of baking temperature on setting time have been investigated in several studies (Dineshkumar and Umarani 2020; Elyamany et al. 2018; Esparham et al. 2020; Nikvar-Hassani et al. 2022). Also, investigations in the field of modulus of elasticity showed that the modulus of elasticity also increased with increasing compressive strength (Esparham and Moradikhou 2021b) (Saravanan and Elavenil 2018) (Nath and Sarker 2017).

The results of one of these studies are summarized in the graphs of Fig. 1. According to the research results, the setting time of GPC is significantly shorter than that of conventional concrete.

Deep learning and machine learning can be used in research to predict the mechanical properties of concrete. Deep learning has the ability to understand the concepts and algorithms between numbers and can help create numerical algorithms and determine the correlation matrix of a set (Hasanzadeh et al. 2022; Rahman and Majumder 2013). In this context, to predict the mechanical properties of high-performance concrete reinforced with basalt concrete fibers, Hasanzadeh et al. found that between the performance of prediction algorithms and the formation of relevant correlation matrices, the linear regression (LR) algorithm is compared to other support vector regression (SVR) algorithms and polynomial regression (PR) is better and has achieved more reliability (Hasanzadeh et al. 2022).

Considering the mentioned materials and the challenges in the production of environmentally friendly active alkaline concrete (geopolymer), this experimental research was carried out with the aim of improving and comprehensively investigating the mechanical properties and durability of active alkaline concrete. It should be noted that concrete geopolymer (GPC) was activated by alkaline solutions of potassium hydroxide and sodium hydroxide together with sodium silicate, as well as a combination of KOH and NaOH (with different percentages to achieve optimal properties), and for curing the manufactured samples, temperatures of 90 degrees Celsius and room temperature (25 °C) were considered for 24 h. GPC samples were prepared in accordance

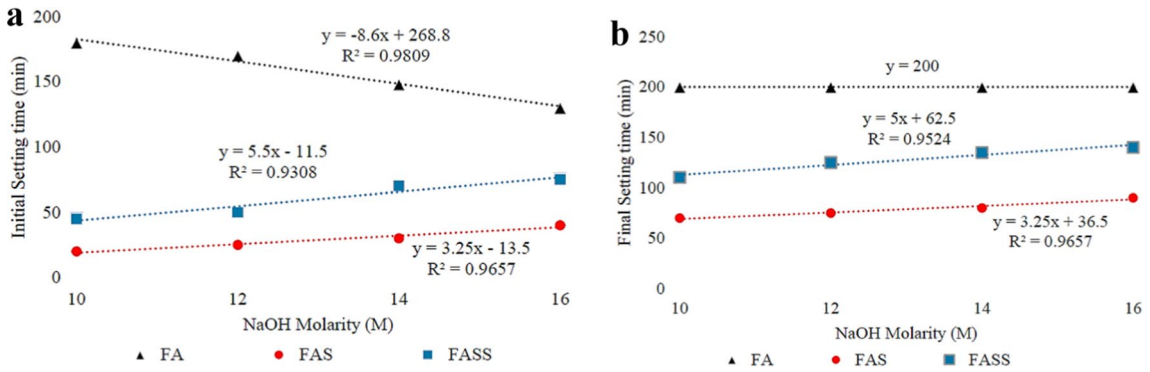

Fig. 1 Changes in time: **a** primary, **b** secondary with changes in base material (Elyamany et al. 2018)

Table 1 XRF analysis of slag

LOI	Cl	SO3	MnO	MgO	K2O	Na2O	Fe2O3	CaO	Al2O3	SiO2	Chemical analysis
0.5	0.02	1.2	1.58	9.8	0.68	0.62	0.6	37.2	11.2	34.4	wt.%

Table 2 Sieve analysis

Sieve analysis									
Coarse aggregates				Fine aggregates					
Sieve (mm)	19	9.5	4.75	4.75	2.36	1.18	0.6	0.3	0.15
Percent Passing	100	45	7.2	100	100	99.8	78.2	25.6	3.5

Table 3 Specifications of the aggregate used in the samples

Fine aggregates	Coarse aggregates	Properties
1.62	6.8	Fineness modulus
97%	38%	Absorption

with the design of the mixtures obtained in the continuation of the research. Also, in order to obtain mechanical properties, the amount of impact energy absorption was calculated from GPC samples, compression, flexural, tensile and impact tests, and then, the samples were used to check the durability properties, including water absorption, water penetration depth and chloride ion penetration depth. Accelerated and carbonation were tested. Finally, the test results were collected, analyzed and reported. Also, in this research, in addition to conducting the relevant tests, the conformity of compressive, tensile and flexural strength results was checked and the modulus of elasticity was measured with common regulations (for the purpose of design and use in the structure) using the correlation matrix.

Materials and methods

In this research, the slag of Isfahan Iron Smelting Furnace was used as the raw material. Slag was purchased from Isfahan Zob Ahan Company, whose XRF analysis is shown in Table 1. For this purpose, NaOH with 98% purity and KOH with 90% purity and liquid Na_2SiO_3 with a weight ratio of SiO_2 to Na_2O equal to 2 were used to prepare alkaline activating solutions from Merck. The specifications of the aggregates used are given in Table 2 and 3. Also, superplasticizer (SP) was used to reduce water in the mix plan and increase the efficiency of the concrete. The water used was the tap water of the city of Tehran.

Mixing procedure

Within the to begin with part, the impact and comparison of the sort of alkaline activator solution on the compressive strength of the fabricated samples have been examined. For this purpose, first, 5 mixing designs of N, K, T-K50N50, T-K80N20 and T-N80K20 are considered with the characteristics listed in Table 4. The concentration of all solutions is 12 mol, and the weight ratio of Na2SiO3 solution to hydroxide solution is considered equal to 1 in all designs. Also, in all designs, the weight ratio of alkaline solution to slag is assumed to be 0.5. The ratio of sand to gravel is assumed to be 1.

First, NaOH and KOH solutions of M12 concentration were prepared. In the designs N, K, T-K50N50, T-K80N20 and T-N80K20, hydroxide solutions were added to the Na_2SiO_3 solution according to the mixed designs 24 h before the test. On the day of the test, dry materials including slag, sand and sand were dry mixed for 3 min, then alkaline activator solution and SP were added to the mixture according to the mixing schedules, and concrete was mixed for 10 min. After mixing, the GPC samples were shaped and compacted. At this stage, the samples were processed in two ways (one at 90 °C for 24 h and the other at room temperature (25 °C) for 24 h). Then 7- and 28-day compressive strength tests were performed on the GPC samples according to BS1881: Part 116 (B. Standard 1983). In the second part of this study, to study the effect of the concentration of NaOH and KOH solution on the compressive strength of GPC and to achieve the optimal concentration, eight different mixing designs were considered, shown in Table 4.

As given in Table No. 4, different concentrations have been used in KOH or NaOH solutions, which include 8, 10, 12 and 14 M. It should also be noted that the weight ratio of Na2SiO3 solution to KOH and NaOH is assumed to be 1.5. In this mixing designs, the percentage of sand is the same and other values are the same as the first case. After preparing the samples and curing them at 90 °C and 25 °C, we prepare the samples for the 7-day and 28-day compressive strength test, and they are subjected to the compressive strength test. We are based on the BS1881: Part 116 standard.

In the next part of this study, the optimal ratio of sodium silicate to hydroxide solution is examined. For this purpose, 8 mixing plans according to Table 5 were considered.

Table 4 First part mixture design

Mix ID	Slag	NaOH 12M	KOH 12M	Na2SiO3	Coarse aggregates	Fine sand	SP	Unit	Weight ratio of Na2SiO3 to KOH and NAOH
N	400	100	0	100	840	840	8	Kg/m3	1
K	400	0	100	100	840	840	8	Kg/m3	1
T-K50N50	400	50	50	100	840	840	8	Kg/m3	1
T-N80K20	400	80	20	100	840	840	8	Kg/m3	1
T-K80N20	400	20	80	100	840	840	8	Kg/m3	1
KR 1.5	400	0	80	120	840	840	8	Kg/m3	1.5
KR 2	400	0	65	135	840	840	8	Kg/m3	2
KR 2.5	400	0	57	143	840	840	8	Kg/m3	2.5
KR 3	400	0	50	150	840	840	8	Kg/m3	3
MR 1.5	400	80	0	120	840	840	8	Kg/m3	1.5
MR 2	400	65	0	135	840	840	8	Kg/m3	2
MR 2.5	400	57	0	143	840	840	8	Kg/m3	2.5
MR 3	400	50	0	150	840	840	8	Kg/m3	3

Table 5 Mixer design to achieve optimal hydroxide concentration

Mix ID	Slag	KOH	NaOH	Na_2SiO_3	Coarse aggregates	Fine sand	SP	Unit	Molarity
K8	400	80	20	120	840	840	8	Kg/m^3	8
K10	400	80	20	120	840	840	8	Kg/m^3	10
K12	400	80	20	120	840	840	8	Kg/m^3	12
K14	400	80	20	120	840	840	8	Kg/m^3	14
N8	400	20	80	120	840	840	8	Kg/m^3	8
N10	400	20	80	120	840	840	8	Kg/m^3	10
N12	400	20	80	120	840	840	8	Kg/m^3	12
N14	400	20	80	120	840	840	8	Kg/m^3	14

In the last part, the analysis and comparison of the type of alkaline activation solution on compressive, flexural and tensile strength were performed based on the results of the previous steps. For this purpose, 5 designs N, K, T-K50N50, T-K80N20 and T-N80K20 are considered. In this part, the concentration of all solutions is equal to 12 and 8 mol (optimal concentration and lowest concentration), and also, the weight ratio of Na2SiO3 solution to hydroxide solution is equal to 1.5 in all designs, and the weight ratio of lye to slag is equal to 5. Sand to sand is considered equal to 1. Following the previous steps, the samples were cured at 90 °C and room temperature (25 °C) for 24 h to calculate the 7-day and 28-day compressive strength according to BS1881: Standard Part 116, 7- and 28-day flexural strength. Based on ASTM C293 standard (Testing and Materials, 2001a) and the indirect tensile test (Brazilian) is performed based on ASTM C09 (A. I. C. C. o. Concrete and Aggregates, 2017). It should be noted that the dimensions of the bending specimens are 10*10*40 cm and the dimensions of the cylindrical tensile specimens are 20*10 cm. The mixing schedules at this stage are given in Table 6.

In addition, the modulus of elasticity was measured according to the procedure of ASTM C469/C469M-10 (A. Standard 2010) for cylindrical samples 10 cm in diameter and 20 cm in height. The test was performed for 3 designs N, K, N80k20 and 3 cylindrical specimens were used for each design (Fig. 2).

Slump test

In this research, the slump test was performed to determine the psychoactivity and design applicability of polymer concrete mixes according to the standard BS EN 12350–2 (EN, 2009). Also the apparatus of this test, which is an incomplete cone, and the implementation of the settling test are shown in Fig. 3.

Table 6 Mixed design of the last part

Mix ID	Slag	NaOH 12 M	KOH 12 M	Na2SiO3	Coarse aggregates	Fine sand	SP	Unit
N	400	80	0	120	840	840	8	Kg/m^3
K	400	0	80	120	840	840	8	Kg/m^3
T-K50N50	400	40	40	120	840	840	8	Kg/m^3
T-N80K20	400	65	25	120	840	840	8	Kg/m^3
T-K80N20	400	25	65	120	840	840	8	Kg/m^3
Mix ID	Slag	NaOH 8 M	KOH 8 M	Na2SiO3	Coarse aggregates	Fine sand	SP	Unit
N	400	80	0	120	840	840	8	Kg/m^3
K	400	0	80	120	840	840	8	Kg/m^3
T-K50N50	400	40	40	120	840	840	8	Kg/m^3
T-N80K20	400	65	25	120	840	840	8	Kg/m^3
T-K80N20	400	25	65	120	840	840	8	Kg/m^3

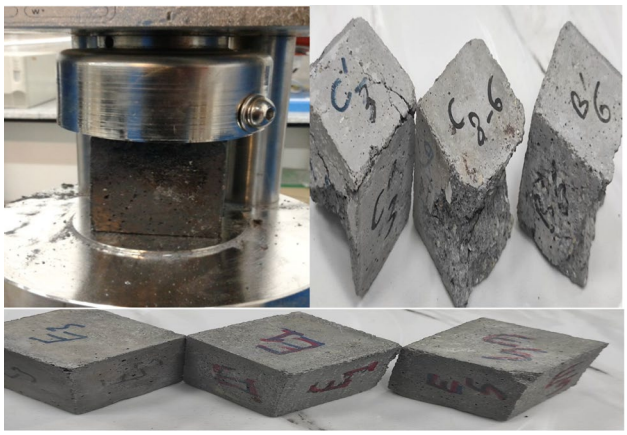

Fig. 2 Samples of prepared concrete

Fig. 3 Slump test

Impact resistance test of falling weight

The falling weight impact test is one of the tests that determine the mechanical properties of concrete. There is no standard method for determining the impact strength of concrete. Projectile impact test, Sharpie test, falling weight test and Hopkinson stick test are sequential tests proposed by the ACI 544-2R committee (Ahmad 1998) to verify the impact performance of concrete. In the repeated impact drop weight tester, the number of impacts is achieved to produce a specified breaking strength, which is a measure of the energy absorption capacity of the material. This test is conducted by dropping a 4.54 kg weight from a height of 457 mm and applying repeated impacts until specified levels of cracking (initial cracking and final cracking) persist. This test was carried out on concrete samples with disk dimensions of 15 × 16.36 cm obtained from GPC on the basis of blast furnace slag treated at ambient temperatures of 25 °C and 90 °C aged 28 days, and also based on Eq. (1), calculation of impact energy absorption capacity is performed, where N is the number of impacts causing the initial crack, W is the weight of the hammer and H is the height of fall (Chen et al. 2023).

$$E = N(WH) \tag{1}$$

Correlation matrix

The meaning of correlation between two variables is to measure the amount of prediction of the values of one based on the other. In other words, the higher the correlation coefficient, the higher the possibility of predicting the value of one of the variables in terms of the other. Correlation matrix by showing the degree of relationship between variables causes the formation of clusters so that the variables within each cluster are correlated with each other, but there is no correlation between the variables in different clusters.

The correlation coefficients according to Pearson and Spearman are between 1 and -1. In this way, when the correlation coefficient is close to or equal to 1, there is a strong relationship and the same direction between the two variables. In this case, it can be said that the direction of change of both variables is similar. This means that as one increases, the other also increases. This relationship

is also based on reduction, i.e., if one of the variables is reduced, the other is also reduced. In this case, one speaks of a direct relationship between two variables (Hasanzadeh et al. 2022; Rahman and Majumder 2013).

Concrete water absorption test

One of the important properties of concrete against environmental influences and durability is the water absorption of the concrete. The lower the water absorption of the concrete, the lower the possibility of harmful ions penetrating the concrete, and eventually reinforcement corrosion or destruction will be reduced. To perform this test according to ASTM C642 standard (Testing and Materials, 2001b), $100 \times 100 \times 100$ mm cubic GPC samples after 28 days of processing were first dried in a heater with a temperature of 105 degrees Celsius for 72 h. Is. After this time and cooling the samples in the laboratory environment, first their weight is measured, and then, the samples are put in water and their wet weight after half and 24 h is measured and the water absorption of the samples is calculated in the mentioned times.

Water penetration depth test

According to the standard DIN 1048-Part 5 (fur Normung, 1991), to carry out this test, cubic specimens of 150*150*150 mm are placed in the testing machine after 28 days of processing and the specimens in the machine are subjected to a pressure of 5 atmospheres for 72 h exposed. After this time, the samples are taken out of the machine and broken with a pressure jack, and the depth of water penetration into the concrete is measured. The apparatus of this experiment is shown in Fig. 4.

Fig. 4 Water penetration depth test

Rapid chloride permeability test

Chloride ion penetration into concrete is known as the most destructive factors of concrete structures, therefore determining the amount of chloride ion penetration is of particular importance (Mousavinejad and Sammak 2021). To measure the resistance of the samples to chloride ion penetration, the accelerated chloride ion penetration test was performed on the samples at 28 days of age. This test is based on the ASTM C1202 standard (C, A 2012). This test measures the amount of flux passed in Coulomb units, thereby qualitatively determining the specimen's resistance to penetration by chloride ions. According to the standard of this test, an impregnated concrete disk, 100 mm in diameter and 50 mm thick, is subjected to 60 V DC for 6 h. A 3% NaCl solution is poured into one tank of the machine and a NaOH solution with a concentration of 0.3 M is poured into the other tank, and then, the total flow through the concrete is measured.

Carbonation test

Carbonation is the reaction between the carbon dioxide penetrated into the concrete and the alkaline products that result from the hydration of the cement in the concrete and the production of calcium carbonate (Mousavinejad and Sammak 2021). To determine the resistance of the prepared samples to carbonation, a chamber connected to a CO2 gas capsule was used as shown in Fig. 5. In order to determine the carbonation depth more quickly, for the environmental

Fig. 5 Carbonation test devices

conditions of the tank, the CO2 concentration is 40.1%, the relative humidity is 655%, and the temperature is 223 degrees Celsius. The depth of infiltrated CO2 was measured according to the RILEM CPC-18 standard (Commitee 1984) using a Phenolphthalein detector dissolved in ethanol alcohol.

Results and discussion

Slump

Depending on the concentration of the active ingredient and the relevant ratios, the flowability of GPC is between 110 and 135, and the flowability or workability of GPC also affects the properties of fresh concrete (Meesala et al. 2020). Investigations have shown that as the molarity of NaOH increases, the workability decreases (Lokuge et al. 2018; Mehta et al. 2017; Ranjbar et al. 2020; Shadnia et al. 2015). The results of the slump test of geopolymer concretes are shown in the diagram of Fig. 6. Depending on the design of the mixtures used, the results obtained for the slump of geopolymer concretes show that the samples containing KOH have more slump (more fluidity) than the samples containing NaOH. The cause of this phenomenon is due to the different reactivity of these two substances. Because KOH has a larger atomic radius than NaOH, it reacts more slowly and requires more activation energy. On the other hand, the initial setting time is delayed in the geopolymer gelation process. Also, the results show that with the increase in the concentration of NaOH and KOH solutions, the amount of slump and workability decreases, which is because the amount of water in the solution decreases with the increase in concentration (Esparham 2022a, b; Nguyen et al. 2020; Sipos, Hefter, and May, 2000; Tennakoon et al. 2016; Verma and Dev 2021) (Fig. 7).

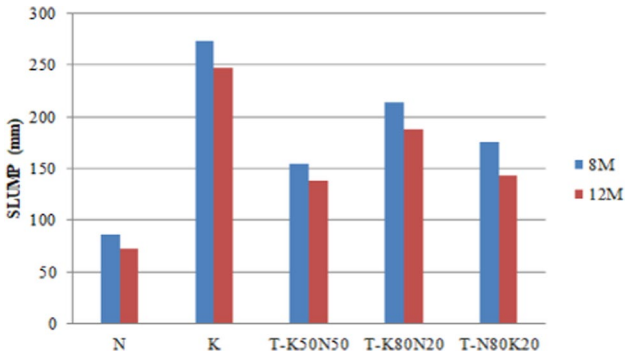

Fig. 6 Effect of different combinations of alkaline activation solutions with concentrations of 8 and 12 M on slag-based GPC slump

Impact resistance test of falling weight

The amounts of impact energy to reach the first crack and the final crack are shown in Table 7 and 8. Samples made at a curing temperature of 90 degrees Celsius have higher impact resistance than samples cured at room temperature. For example, the increase in fracture energy absorption strength of samples from K to N80K20 (12 M) is 18, 19, 16, 18 and 27%, respectively, for samples cured at 90 °C

Table 7 GPC 8 M crack impact energy at different temperatures

Sample	First crack		Ultimate crack	
	25o C	90O C	25o C	90O C
K	16	20	154	208
N	21	28	229	270
T-K50N50	12	17	125	176
T-K80N20	17	21	173	252
T-N80K20	24	30	288	321

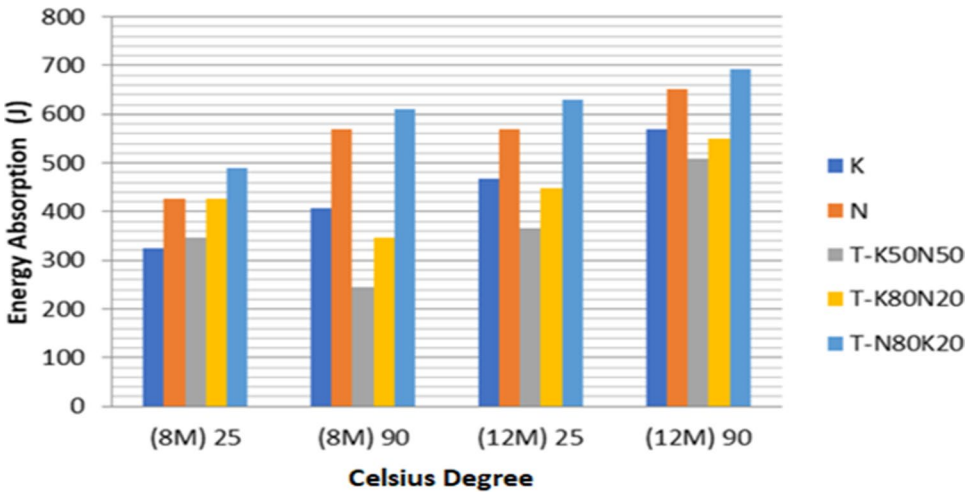

Fig. 7 Energy absorption (impact) in the first moment of cracking

Table 8 GPC 12 M crack impact energy at different temperatures

Sample	First crack		Ultimate crack	
	25o C	90O C	25o C	90O C
K	23	28	239	291
N	22	27	230	281
T-K50N50	18	25	218	260
T-K80N20	28	32	270	333

compared to those cured at room temperature (Fig. 8). In this regard, the greatest increase in strength is related to the N80K20 sample (cured at 90 °C). According to the results, it can be said that the high activation energy and the reaction tendency of potassium to form very dense oligomers (in the geopolymer matrix) and the high dissolution rate of sodium compared to potassium in alumina silicate gel lead to the dissolution of Al2O3 and SiO2 in raw materials in solution. It becomes active. These reasons can lead to greater continuity of bonding in the joint transition area and the formation of a stronger structure of hydrated gels and greater participation of particles in the geopolymerization process, which in turn improves the adhesion between particles at a curing temperature of 90 °C (Esparham 2022a, b; Shilar et al. 2022; Sipos et al. 2000).

Compressive, tensile and flexural strength

Factors influencing the compressive strength of active alkali concrete (geopolymer) include the type of raw materials and the type of activating solution. In this research, the effect of KOH and NaOH solution concentration on compressive, tensile and bending strength is shown in graphs 9, 10, 11 and Tables 9, 10, 11 and 12. As shown in Fig. 9a, b, by increasing the concentration of KOH and NaOH solutions, the compressive strength of 7 and 28 days in each curing mode at 90 °C and 25 °C increases up to a concentration of 12 M and then lasts. The decreasing trend and the best ratio of sodium silicate composition to sodium or potassium hydroxide is equal to 1.5 (Figs. 9c, d). According to the results obtained in diagrams 10a, b and 11a, b, it can be seen that in general the tensile and **flexural** strength of concrete samples are directly related to its compressive strength, so the best tensile and bending performance occurred in 12 M concentration (Farooq et al. 2020; Hardjito and Rangan 2005; Noushini et al. 2016). Increasing the molarity of the activating solution increases the dissolution rate of the raw material. As a result, the compressive, tensile and flexural

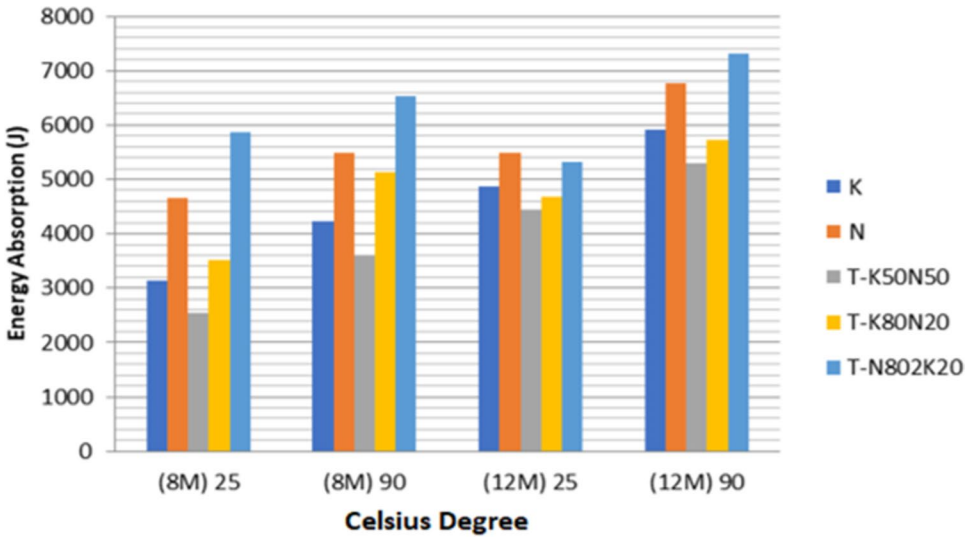

Fig. 8 Energy absorption (impact) in fracture crack

Table 9 Summary table of results obtained for 8 M samples at 90 degrees Celsius

	Compressive strength (MPa)		Tensile strength (MPa)		Flexural strength (MPa)	
	7 days	28 days	7 days	28 days	7 days	28 days
N	63.6 ± 0.1	93.3 ± 0.6	3.5 ± 0.6	5 ± 0.2	5.7 ± 0.4	8.2 ± 0.3
K	52.9 ± 0.3	85.3 ± 0.3	2.9 ± 0.3	4 ± 0.3	4.8 ± 0.6	6.5 ± 0.4
T-K50N50	49 ± 0.2	60 ± 0.3	2.7 ± 0.9	3.3 ± 0.5	4.4 ± 0.4	5.4 ± 0.4
T-K80N20	59.8 ± 0.6	68.7 ± 0.3	3.3 ± 0.3	3.8 ± 0.3	5.4 ± 0.5	6.2 ± 0.2
T-N80K20	96.6 ± 0.1	113.4 ± 0.6	5.3 ± 0.6	6.2 ± 0.1	8.3 ± 0.3	10.2 ± 0.5

Table 10 Summary table of results obtained for 8 M samples at 25 degrees Celsius

	Compressive strength (MPa)		Tensile strength (MPa)		Flexural strength (MPa)	
	7 days	28 days	7 days	28 days	7 days	28 days
N	44.8 ± 0.4	72.3 ± 0.4	2.5 ± 0.4	4.3 ± 0.1	4 ± 0.2	7.1 ± 0.2
K	37.6 ± 0.4	62.2 ± 0.2	2.1 ± 0.5	3.9 ± 0.2	3.4 ± 0.5	5.6 ± 0.5
T-K50N50	35.6 ± 0.4	54.4 ± 0.3	2 ± 0.4	3 ± 0.2	3.2 ± 0.5	4.9 ± 0.3
T-K80N20	42.1 ± 0.4	59.1 ± 0.5	2.3 ± 0.1	3.2 ± 0.1	3.8 ± 0.2	5.3 ± 0.5
T-N80K20	80.5 ± 0.5	96.7 ± 0.3	4.4 ± 0.4	5.3 ± 0.5	7.2 ± 0.2	8.7 ± 0.5

Table 11 Summary table of results obtained for 12 M samples at 90 degrees Celsius

	Compressive strength (MPa)		Tensile strength (Mpa)		Flexural strength (Mpa)	
	7 days	28 days	7 days	28 days	7 days	28 days
N	94.8 ± 0.5	116 ± 0.4	5.2 ± 0.6	6.9 ± 0.1	8.3 ± 0.3	10.9 ± 0.5
K	71.8 ± 0.4	105 ± 0.4	3.9 ± 0.1	5.9 ± 0.6	6.1 ± 0.5	10.2 ± 0.4
T-K50N50	68.2 ± 0.2	94.8 ± 0.3	3.8 ± 0.4	5.2 ± 0.2	5.8 ± 0.5	8.8 ± 0.3
T-K80N20	89.1 ± 0.5	102.3 ± 0.4	4.9 ± 0.6	5.6 ± 0.1	7.9 ± 0.2	9 ± 0.6
T-N80K20	106.2 ± 0.5	127.4 ± 0.3	5.8 ± 0.2	7 ± 0.6	9 ± 0.2	11 ± 0.4

Table 12 Summary table of results obtained for 12 M samples at 25 degrees Celsius

	Compressive strength (Mpa)		Tensile strength (Mpa)		Flexural strength (Mpa)	
	7 days	28 days	7 days	28 days	7 days	28 days
N	74.1 ± 0.4	96.8 ± 0.2	4 ± 0.4	5.9 ± 0.3	6.7 ± 0.4	9 ± 0.4
K	56.9 ± 0.5	84.2 ± 0.2	3.2 ± 0.6	5 ± 0.4	5.1 ± 0.4	7.9 ± 0.4
T-K50N50	54.8 ± 0.5	77.6 ± 0.4	2 ± 0.3	3 ± 0.1	4.9 ± 0.3	7 ± 0.3
T-K80N20	67.8 ± 0.2	88.6 ± 0.3	2.3 ± 0.4	3.2 ± 0.3	6.1 ± 0.2	7 ± 0.5
T-N80K20	90.4 ± 0.3	109.2 ± 0.2	4.4 ± 0.2	5.3 ± 0.6	8.1 ± 0.4	9.8 ± 0.2

strengths increase with the increase in the concentration of the hydroxide solution. The reason for this is that with higher concentrations of Al2O3 and SiO2, the materials in the raw material dissolve faster in the activation solution, and as a result, larger amounts of geopolymer gel are formed, which leads to an increase in compressive strength. The reason for the decrease in compressive strength at concentrations higher than 12 M is that when the concentration of NaOH and KOH increases to 14 M, after a very short time after the start of geopolymerization, more hydroxide ions are precipitated in the aluminate gel. This process delays the subsequent reaction, resulting in reduced the compressive, tensile and flexural strengths (Jan et al. 2022; Rehman et al. 2020).

In the following, according to the test results, the effects of the percentage of KOH and NaOH solutions on the compressive, tensile and flexural strengths of concrete samples are shown in the graphs of Figs. 9f, e, 10c, d, 11c, d. As can be seen in the graphs, the highest compressive, tensile and flexural strength values of 7 and 28 days correspond to the T-N80K20 design, and it can also be seen that the T-K50N50 design is the least. For example, the highest compressive strength values are 7 and 28 days. The day is related to the T-N80K20 mixing design (12 M, curing at 90 degrees Celsius) whose values are 106.2 and 127.4 MPa, respectively, and the lowest compressive strength values of 7 and 28 days are related to the T-K50N50 mixing design (8 M, curing at 25 degrees Celsius) whose values are equal to 35.8 and 54.7 MPa, respectively. These results are due to the much lower activation energy of sodium hydroxide compared to potassium hydroxide and its faster dissolution in aluminosilicate gel, which itself causes the interference of the reactive tendencies of potassium and sodium, which results in a decrease in the degree of polymerization (Jafari Nadoushan and Ramezanianpor 2019). On the other hand, the highest strength value of 7 and 28 days is related to the T-N80K20 design, and from this point of view, it can be said that the T-N80K20 sample has eliminated the interaction effect of sodium and sodium reactivity. Considering the reactivity of potassium to form dense agglomerates, potassium has strengthened the geopolymer matrix to a favorable extent (Esparham and Moradikhou 2021c; Huang et al. 2022; Jafari Nadoushan and Ramezanianpor 2019; Abdelmoamen and Abdelsalam, 2020). The noteworthy point in these graphs is the 7-day compressive strength of the potassium mixing plan (k) compared to its 28-day resistance. The size of sodium ions is 116 pm and that of potassium ions is

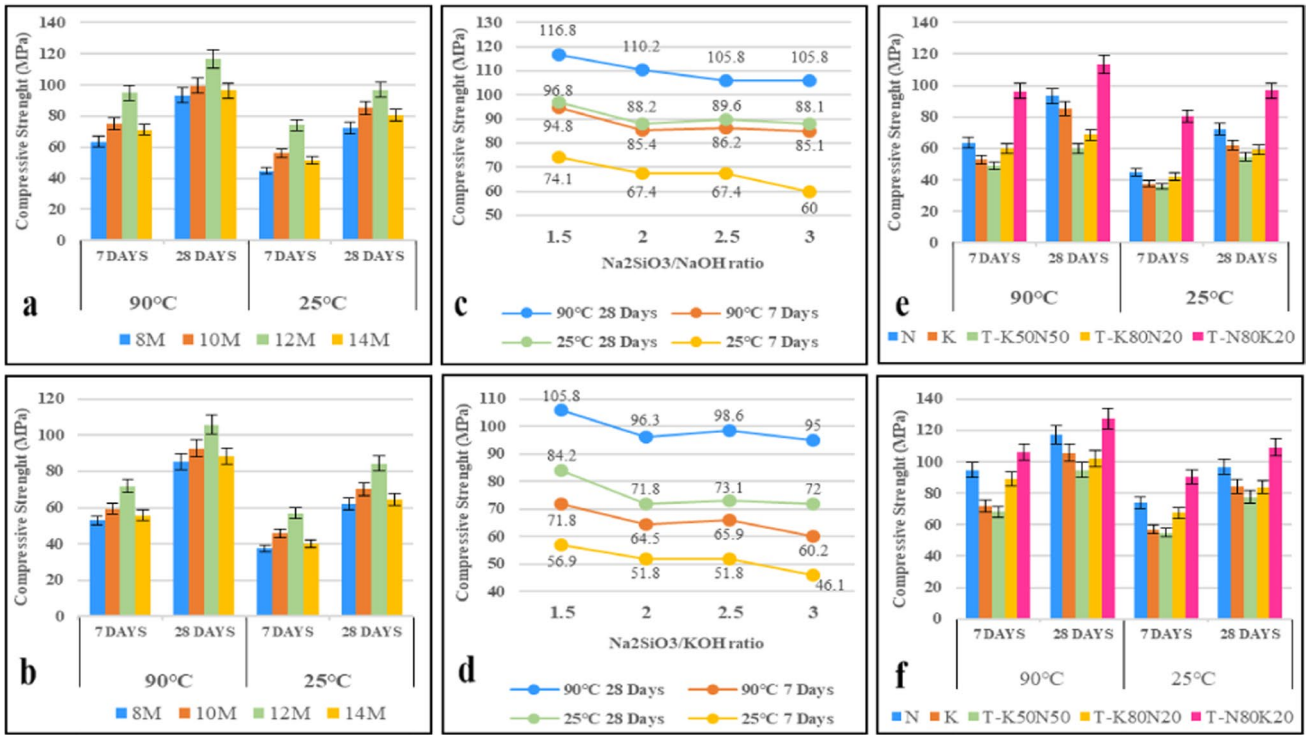

Fig. 9 Compressive strength diagram of samples with **a**. NaOH and **b**. KOH cured at 90 and 25 degrees Celsius and the compressive strength diagram of samples in different proportions of Na2SiO3 with **c**. NaOH and **d**. KOH treated at 90 and 25 degrees Celsius and compressive strength diagram of samples with concentration **e**. 8 M and **f**. 12 M at 90 and 25 degrees Celsius

152 pm. The larger size of potassium ion causes the formation of larger oligomers than aluminum hydroxide, and also because of the need for more activation energy than sodium, it enters the reaction later and dissolves in the aluminosilicate gel, which means that this design is used to achieve Its maximum strength requires more curing time and temperature (Jafari Nadoushan and Ramezanianpor 2019; Sipos et al. 2000; Tennakoon et al. 2016).

Scanning electron microscope (SEM)

Images were taken by scanning electron microscope to compare the structure of GPC samples activated with alkaline solutions of sodium hydroxide (NAOH) and potassium hydroxide (KOH) and the combination of these two solutions (N80K20, 80% sodium hydroxide and 20% potassium hydroxide), and also, to analyze the electron microscope images, Fig. 12 is provided.

The images a and b in Fig. 12 show the formation of gel. Polymerization gels containing the following compounds, hydrated calcium silicate (CSH, hydrated calcium aluminate silicate (CASH) and hydrated sodium and potassium aluminate silicate (K, NA-SH), grab the particles and cover the empty space between them, and they combine the particles together and finally reinforce the geopolymeric network (Lim and Pham 2021; Phoo-ngernkham et al. 2015) In image C, the void space between the holes in the geopolymeric matrix is reduced and finally, in picture d, the sample activated with N80K20 combined solution has the least empty space in the polymerization process compared to other alkaline activating solutions, which increases durability and mechanical properties.

The hardened geopolymer consisting of three paste materials (blast furnace slag, hydroxide solution and sodium silicate) is shown with the letter G in Fig. 13. The number of main cracks in the N80K20 design sample is between 40 and 90 microns, and in the fractured N design sample, the amount of main cracks in Fig. 7 is at least 100 and at most 275 microns. According to the chemical composition of the N80K20 project and eliminating the interference of the reactive desires of sodium and potassium, it was found that the process of these reactions completes the formed geopolymer with fewer and more uniform cracks.

XRD

Samples of the designs that achieved the highest (N80K20) and lowest (N50K50) compressive strength were tested for failure in the X-ray direction. The test results are shown in Fig. 14. The principal materials found in the calcite test

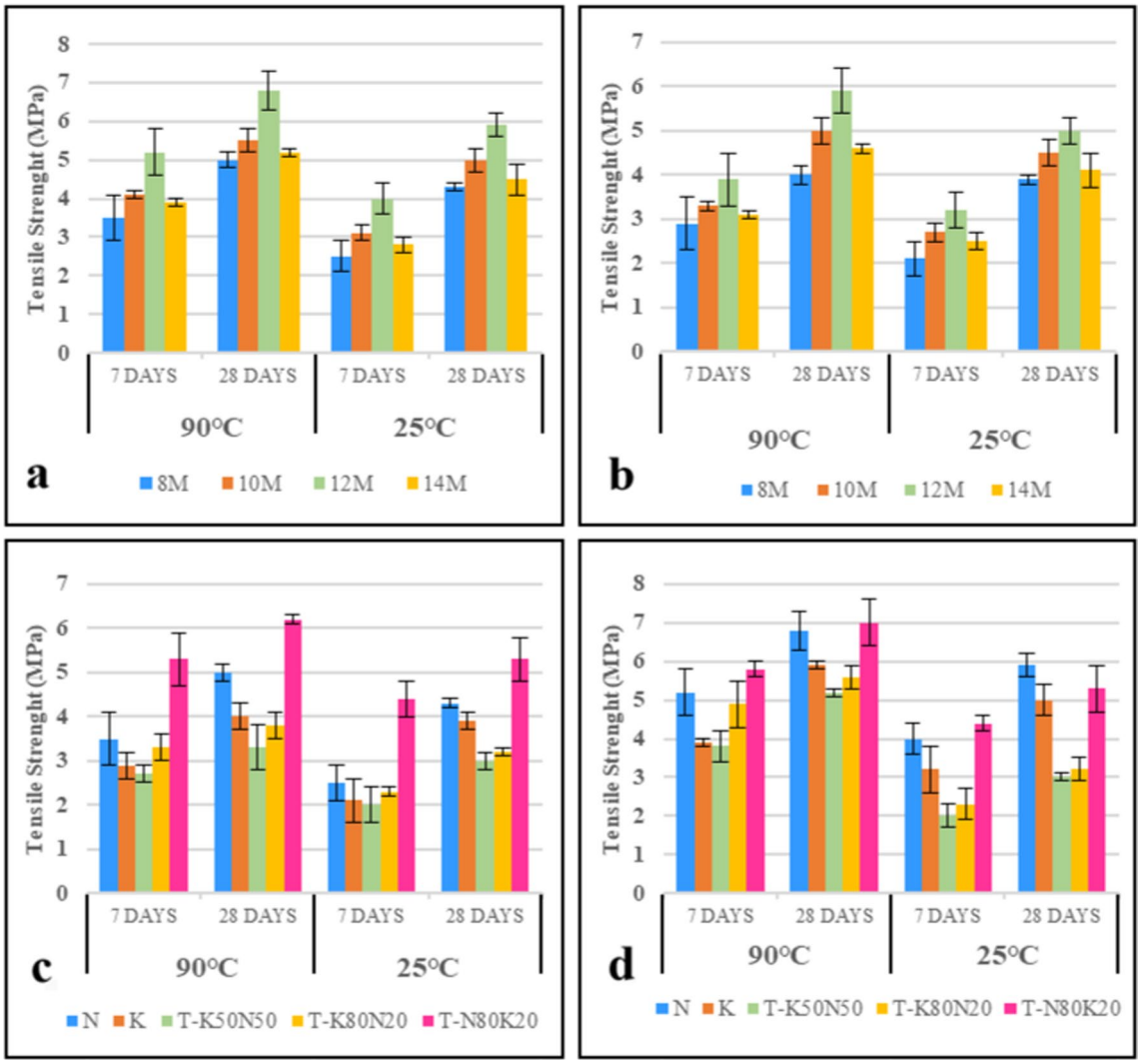

Fig. 10 Tensile strength diagram of samples with **a**. NaOH and **b**. KOH cured at 90 and 25 degrees Celsius and the compressive strength diagram of samples with concentration **c**. 8 M and **d**. 12 M at 90 and 25 degrees Celsius

sample were albite and quartz. As shown in Fig. 14, quartz had the highest intensity of X-ray reflection in both maps. According to the diagram of plan a (N50K50), more intensity of the reflected X-ray was obtained at an angle of 30 degrees (almost twice). This showed that in the N50K50 design the amount of unreacted slag was higher in the geopolymerization process and less resistance was obtained.

Modulus of elasticity

The results are presented in Table 13, 14, 15 and 16, which are also compared with the calculation method of three regulations:

- ACI 363 $Ec28 = 3320\sqrt{fc28} + 6900$ (Russell et al. 1997)
- ACI 318 $Ec28 = 4730\sqrt{fc28}$ (318 and Institute, 1989)
- CEB 1990 $Ec28 = 22{,}000\sqrt{fc28103}$ (F. I. B. I. F. S. Concrete 1990)

The highest and lowest elastic modulus values were calculated to be 50.3 and 36.12 GPa, respectively. Under all conditions, the N80k20 design had the highest Young's modulus, and at a concentration of 12 M and a curing temperature of 90 °C, the designs had the highest Young's modulus. The value of the modulus of elasticity is directly related to the value of the compressive strength (Bellum et al. 2020; Hassan et al. 2022; Ouyang et al. 2020).

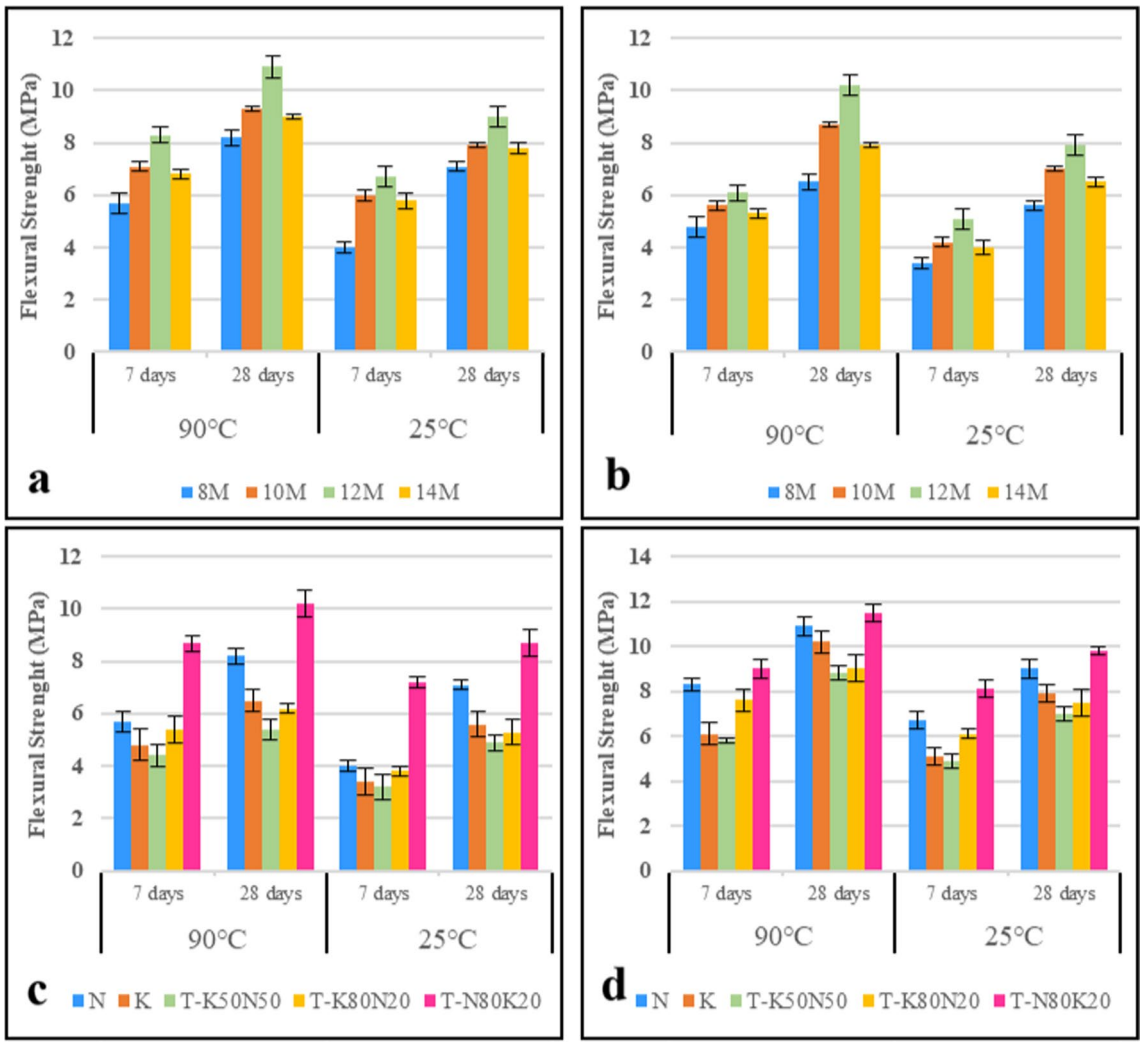

Fig. 11 Flexural strength diagram of samples with **a**. NaOH and **b**. KOH cured at 90 and 25 degrees Celsius and the compressive strength diagram of samples with concentration **c**. 8 M and **d**. 12 M at 90 and 25 degrees Celsius

Correlation matrix

Figure 15 shows that the design N at a concentration of 8 M has the highest correlation with tensile and flexural strength, and after that, T-N80K20 has the highest correlation in such a way that it has a correlation of more than 99% with compression strength at room temperature and the flexural strength has strength.

Like the samples prepared at a concentration of 8 M, the samples prepared at a concentration of 12 M in the N plan had a very high correlation with the resistances. Also, after the N design, the T-N80K20 design had the highest relationship to tensile, flexural and compressive strengths (Fig. 16).

According to Figs. 17 and 18, the best correlation results were obtained for the T-N80K20 design with concentrations of 8 and 12 M and under the condition of curing at room temperature with ACI 363 and ACI 318 regulations and at 90 °C with CEB regulations. Ninety best correlations were obtained for modulus of elasticity.

Durability tests

The durability of any structural component includes the ability to withstand weather conditions, chemical attacks, abrasion or any other destructive process. The most basic and common tests of concrete durability include things such as: water absorption tests, changes in chloride ion penetration depth and carbonation indicated. In the following, we will examine these tests and determine the durability properties of active alkali concrete (Deepak and Lakshmi 2020; Esparham and Moradikhou 2021a; Rehman et al. 2020; Gunasekara et al. 2016).

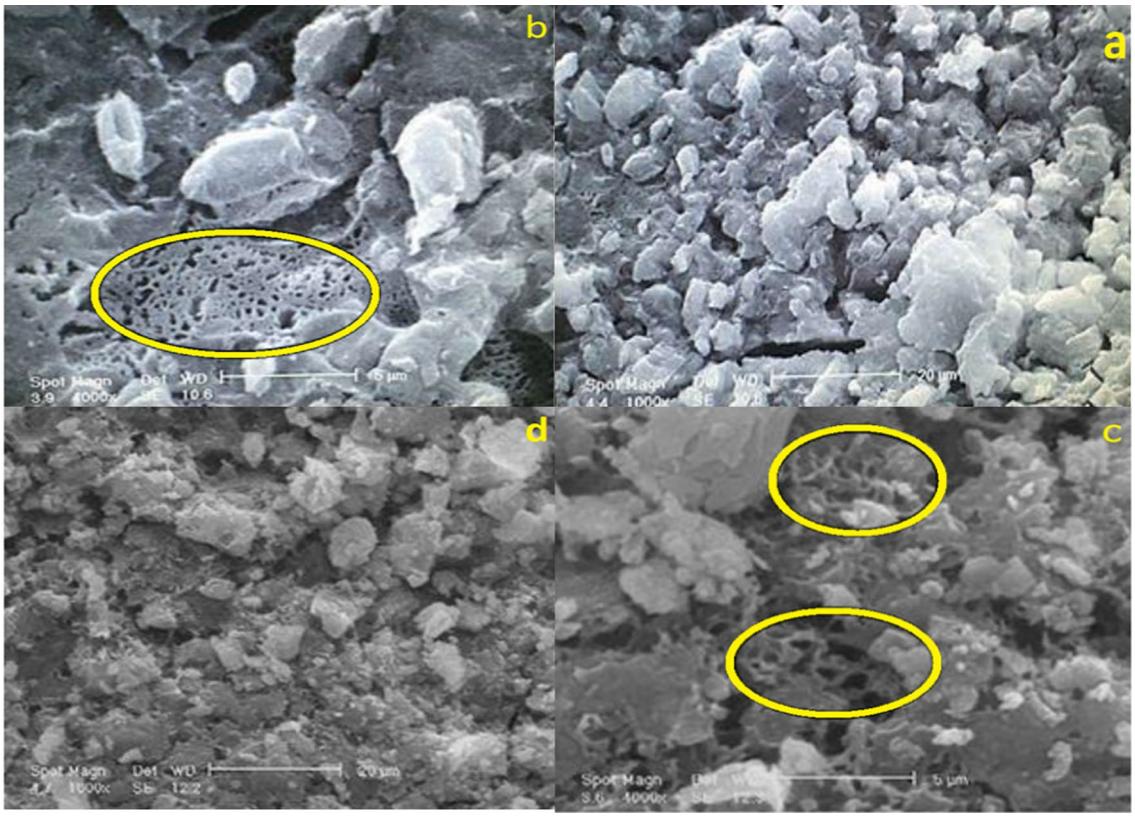

Fig. 12 Comparison of electron micrographs of geopolymer concrete samples activated with alkaline solutions of **a** KOH (scale 20 microns), **b** KOH and **c** NAOH (scale 5 microns), **d** N80K20 (scale 20 microns)

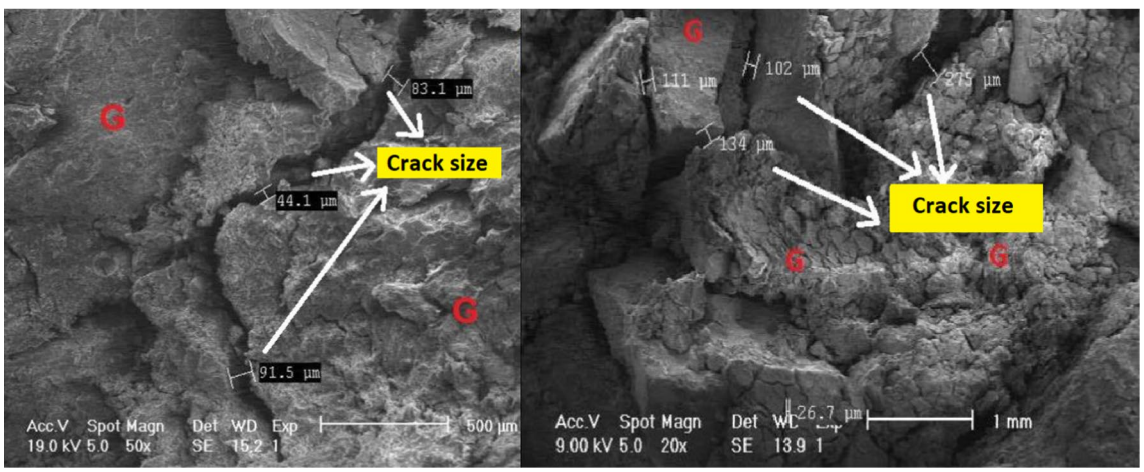

Fig. 13 Electron micrograph taken for fractured samples of N80K20 and N designs

Water absorption tests and water penetration depth of concrete

The results of the concrete water absorption and penetration test results are presented in the graphs of Figs. 19a, b and 20. According to the graphs of the water absorption test, the 12 M samples in both half- and 24-h time groups have less water absorption than the 8 M samples; on the other hand, among the 8 and 12 M samples, the T-N80K20 sample contains 80% of NaOH solution and 20% of KOH solution, it has the lowest water absorption and the lowest water penetration depth, and the highest water absorption

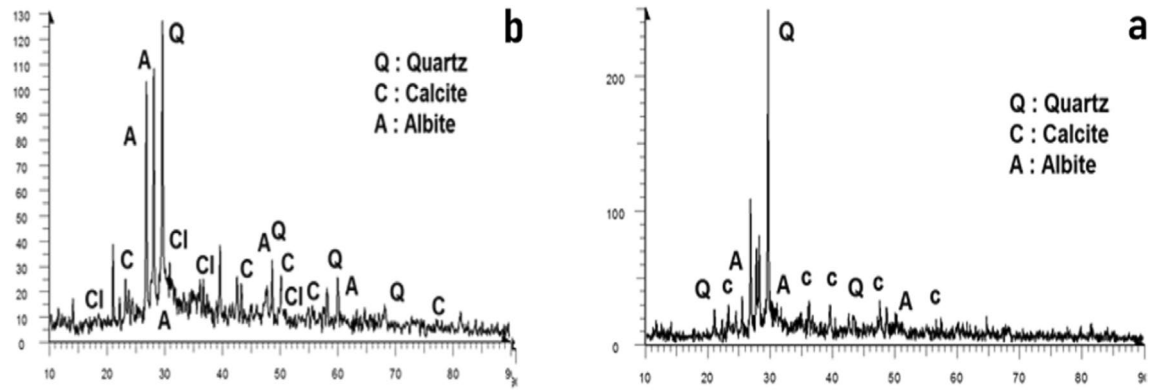

Fig. 14 X-ray test chart for samples of **a** N50K50 and **b** N80K20 designs

Table 13 Modulus of elasticity at a concentration of 8 M and a temperature of 90 °C

Mixture ID	Experimental modulus of elasticity (GPa)		Modulus of elasticity according to ACI 363 (Gpa)	Modulus of elasticity according to ACI 318 (GPa)	Modulus of elasticity according to CEB (GPa)
	Average	Standard deviation			
N	42.83	0.201	38.97	45.69	46.31
K	39.92	0.215	37.56	43.69	44.95
N80K20	45.1	0.278	42.25	50.37	49.43

Table 14 Modulus of elasticity at a concentration of 8 M and a temperature of 25 °C

Mixture ID	Experimental modulus of elasticity (GPa)		Modulus of elasticity according to ACI 363 (Gpa)	Modulus of elasticity according to ACI 318 (GPa)	Modulus of Elasticity according to CEB (GPa)
	Average	Standard deviation			
N	37.28	0.23	35.13	40.22	42.54
K	36.12	0.351	33.08	37.3	40.46
N80K20	43.56	0.297	39.55	46.51	46.87

Table 15 Elastic modulus at a concentration of 12 M and a temperature of 90 °C

Mixture ID	Experimental modulus of elasticity (GPa)		Modulus of elasticity according to ACI 363 (Gpa)	Modulus of elasticity according to ACI 318 (GPa)	Modulus of elasticity according to CEB (GPa)
	Average	Standard deviation			
N	47.23	0.39	42.78	51.12	49.92
K	44.17	0.413	41.05	48.65	48.3
N80K20	50.3	0.313	44.37	53.39	51.38

and water penetration depth in both 8 and 12 M concentrations are related to the T-K50N50 sample. According to the results, it can be seen that by increasing the concentration of the solution (up to 12 M), decreasing the interference of the reactive desires of sodium and potassium ions and increasing the alkalinity, more Al2O3 and SiO2 are dissolved in the polymerization process and more geopolymeric gel is created. These gels fill more capillary holes in concrete,

Table 16 Young's modulus at a concentration of 12 M and a temperature of 25 °C

Mixture ID	Experimental modulus of elasticity (GPa)		Modulus of elasticity according to ACI 363 (Gpa)	Modulus of elasticity according to ACI 318 (GPa)	Modulus of elasticity according to CEB (GPa)
	Average	Standard deviation			
N	43.97	0.321	39.56	46.54	46.89
K	39.26	0.255	37.36	43.4	44.76
N80K20	44.93	0.262	41.59	49.43	48.81

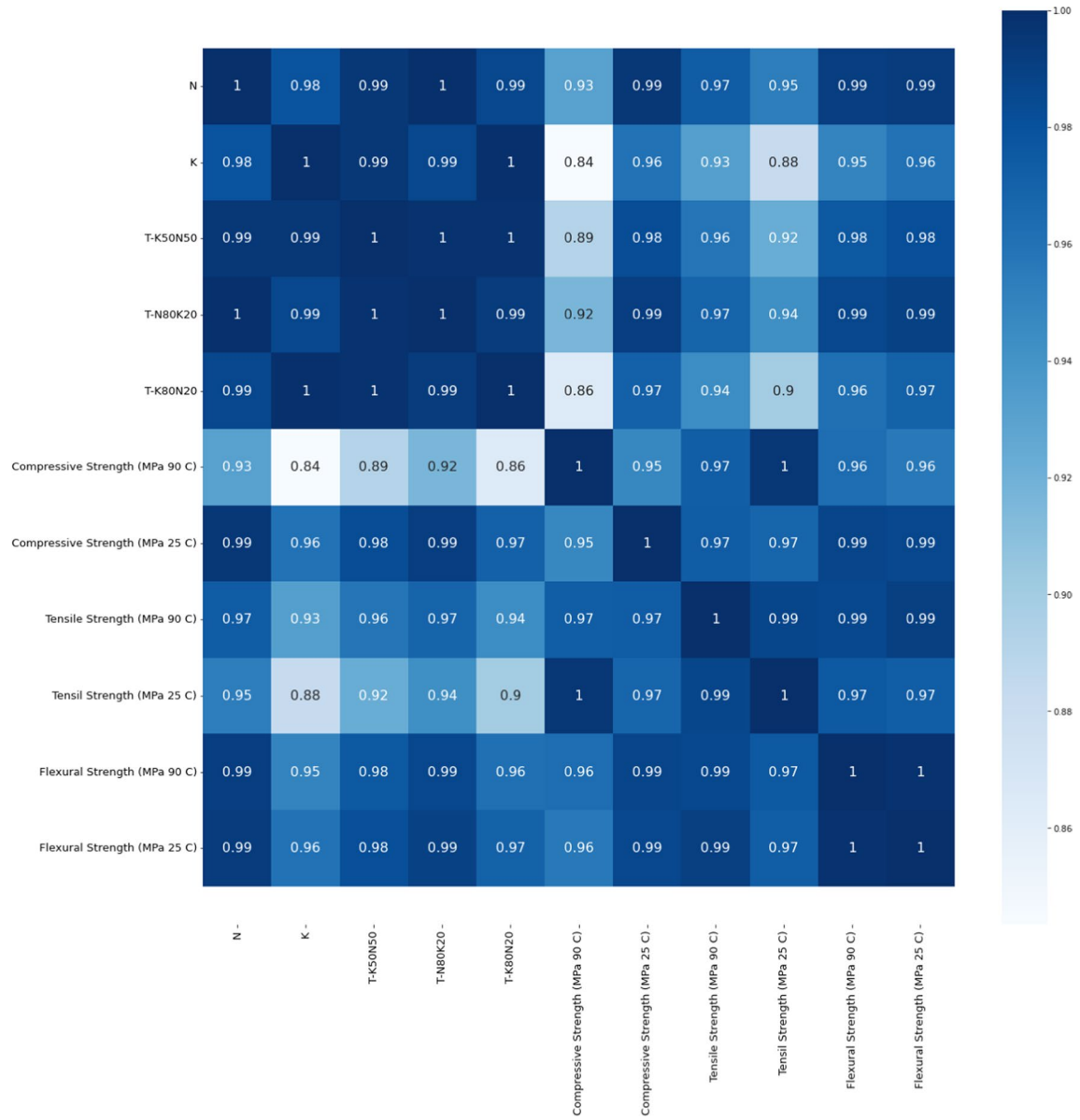

Fig. 15 Correlation matrix for geopolymer concrete with a concentration of 8 M

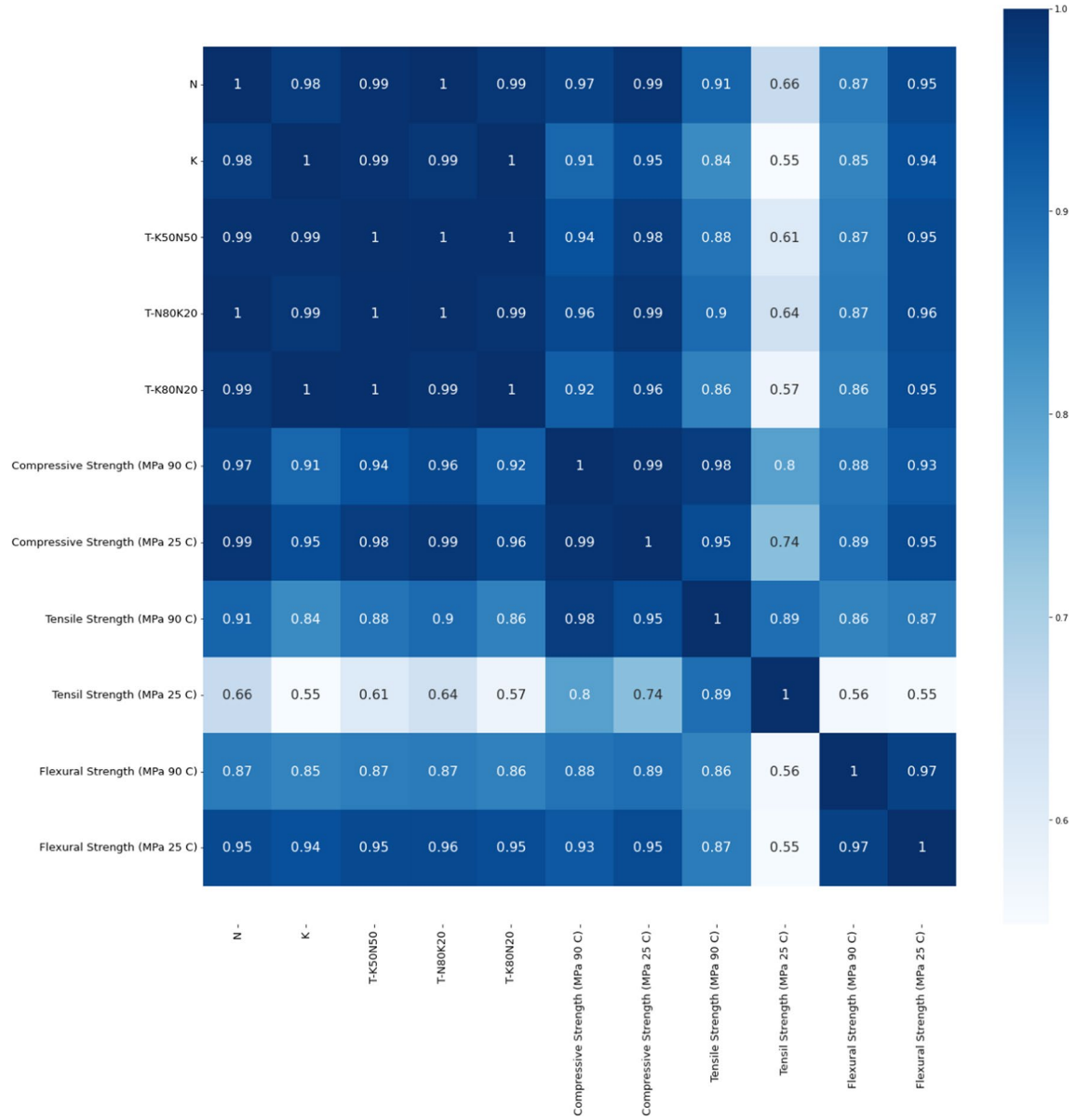

Fig. 16 Correlation matrix for geopolymer concrete with a concentration of 12 M

and ultimately less water absorption and penetration depth are observed in concrete (Amran et al. 2021; Esparham and Moradikhou 2021c; Olivia et al. 2008; Quang Minh et al. 2019; Jindal et al. 2018; Li et al. 2022).

Rapid chloride permeability test

Therefore, it is important that in marine environments, chloride ion penetration into concrete and rebar corrosion damage is known to be the most important destructive factor in concrete structures, with determining the amount of chloride ion penetration being of particular importance (Mousavinejad and Sammak 2021). Figure 21 shows the results of the accelerated chloride ion permeation test, which shows that as the concentration increases from 8 to 12 M, the values of the flux passing decrease, and therefore, the resistance to chloride ion permeation increases. According to the obtained results, it can be seen that the samples (1) T-K50N50, (2) T-K80N20, (3) K, (4) N and (5) T-N80K20, respectively, have the maximum values of the passage flux. This test measures the amount of flux passed in Coulomb units, thereby qualitatively determining the specimen's resistance to penetration by chloride ions. The results of the accelerated chloride ion permeation test show that as the concentration and processing temperature of the constructions increases, due to the production of more gel, the amount of flux that

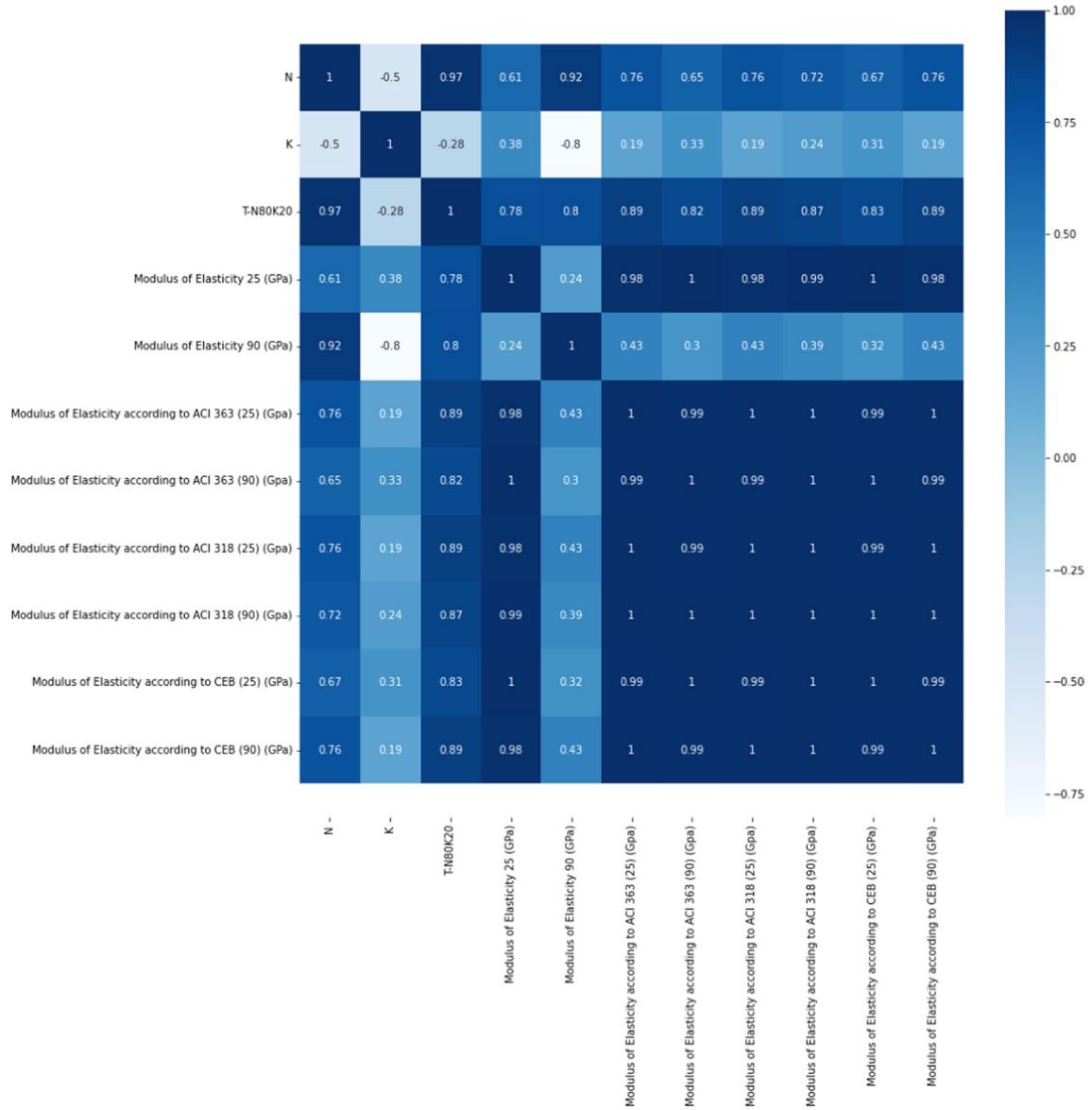

Fig. 17 Correlation matrix for elastic modulus of geopolymer concrete with a concentration of 8 M

passes through decreases, and therefore, the resistance to chloride ion penetration increases (Chindaprasirt and Chalee 2014; Jindal et al. 2018; Noushini and Castel 2018).

Carbonation test

The carbonization test was conducted as the fourth step of the durability test. Carbonation of concrete is a chemical reaction between carbon dioxide penetrated into concrete and alkaline products resulting from hydration of cement in concrete and production of calcium carbonate. CO_2 infiltration reduces the alkalinity of the concrete and destroys the alkaline protective layer around the reinforcement, exposing the test equipment to corrosion (Fig. 22). Carbonation test results are shown in the graphs of Fig. 23 and Table 17. The lowest depth of carbonation value at 14 and 28 days is for the T-N80K20 blend at a concentration of 12 M and treated at 90 °C, and the highest depth of carbonation value is for the T-K50N50 blend at a concentration of 8 M and treated at 25C. From the obtained results, it can be seen that samples with a higher alkaline solution concentration show a lower carbonation depth value compared to samples with a lower alkaline solution concentration. This may indicate an increase in the degree of geopolymerization, a decrease in pores and higher density of the structure and a decrease in the corrosion potential of reinforcing bars in geopolymer concrete samples at

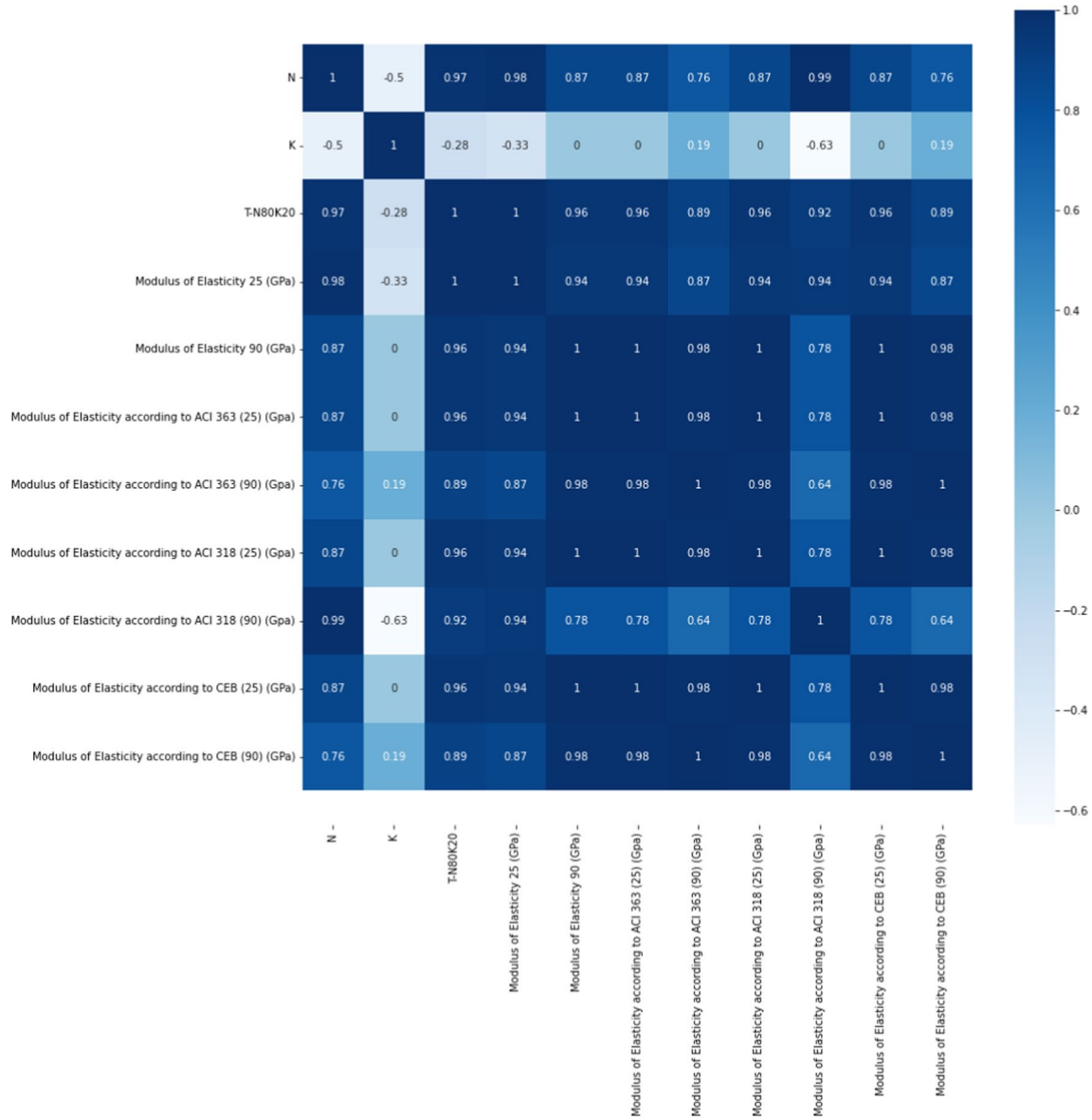

Fig. 18 Correlation matrix for elastic modulus of geopolymer concrete with a concentration of 12 M

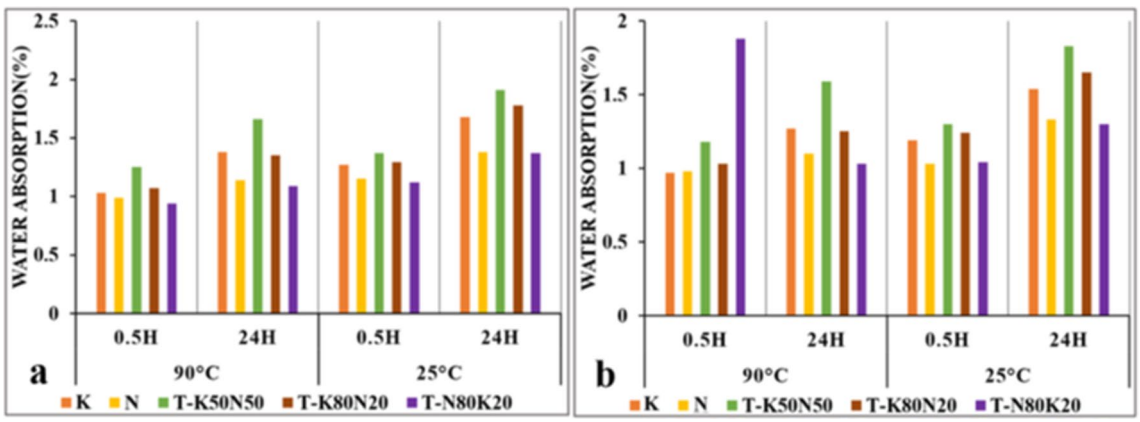

Fig. 19 Half- and 24-h water absorption plots of samples **a**. 8 M and **b**. 12 M and percentage cured at temperatures of 90 and 25 degrees Celsius

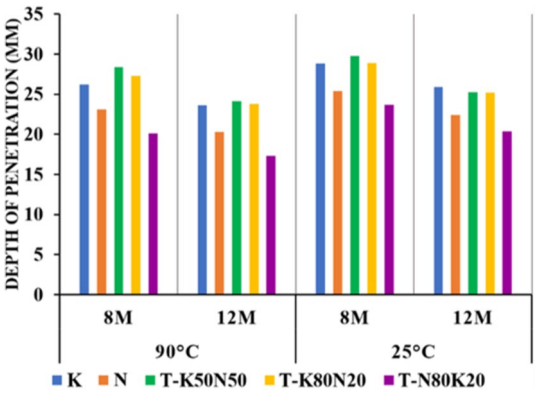

Fig. 20 Plot of penetration depth of 8 and 12 molar samples cured at 90 and 25 degrees Celsius

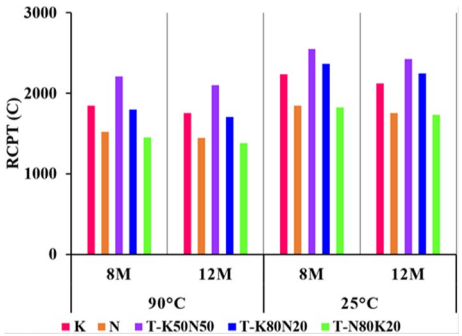

Fig. 21 RCPT plot of 8 and 12 M samples cured at 25 and 90 degrees Celsius

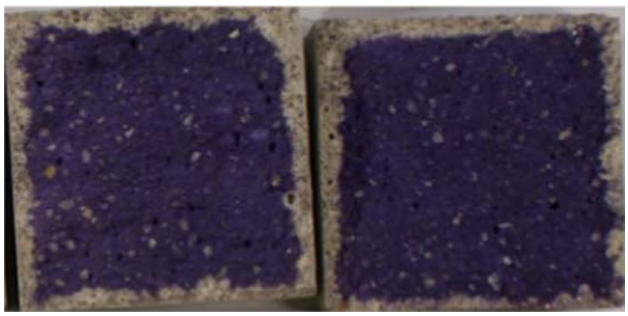

Fig. 22 Carbonated samples

higher concentration and processing temperature (Khan et al. 2017; Pasupathy et al. 2021; Zhuguo and Sha 2018).

Conclusion

According to the results obtained in this investigation, it can be said that the samples containing KOH show more slump than the samples containing NaOH and are therefore more workable. By increasing the concentration of NaOH and KOH solution, the amount of slump and workability decreases. In terms of impact resistance (energy absorption rate), the samples that were cured at 90 degrees Celsius had more energy absorption compared to the samples that were cured at room temperature, and among the prepared samples, the N80K20 design had the highest gained increased impact resistance. In the comparison section, KOH + Na2SiO3 solution with NaOH + Na2SiO3 solution as GPC alkaline activation solution. In relation to the slag, the use of NaOH + Na2SiO3 results in a higher 28-day compressive strength. The use of NaOH + Na2SiO3 leads to an increase in 7-day compressive strength and an early compressive strength. Also, the simultaneous use of the combination of NaOH and KOH + Na2SiO3 solutions as an alkaline activator solution for slag-based geopolymer concrete leads to a significant reduction in the compressive strength of 7 and 28 days due to the disruption of the reactivity of Na + and K + . On the other hand, the optimum concentration of KOH and NaOH solution is 12 mol, and increasing the concentration above this value reduces the mechanical strength of the samples. Samples cured at 90 °C have higher mechanical strength than samples cured at room temperature. Among the prepared samples, the T-N80K20 sample eliminated the interference of sodium and potassium reactivity to an optimal extent, and considering the reactivity of potassium to form larger hydroxide oligomers and the rapid dissolution of sodium in aluminosilicate gel, it can be seen that the resistance The mechanical strength of T-N80K20 sample in 7 and 28 days is more than other mixing designs.

Compared to other mixing designs, the N80k20 design (12 M concentration) has the highest Young's modulus. In chloride ion penetration (accelerated) and carbonation depth tests, it can be said that absorption values, water penetration depth and flow flux of GPC samples decrease with increasing solution concentration and curing temperature. According to the mentioned result, the lowest amount of water absorption, the depth of water penetration, the depth of carbonation, and the chloride ion penetrating flux are related to the N80K20 mixing design. In other words, the N80K20 design outperformed other mixing designs in terms of durability.

In terms of the correlation matrix of the elasticity modulus, the T-N80K20 mixing design with 8 and 12 M concentrations and at a curing temperature of 90 degrees Celsius with the CEB 90 regulation and at room temperature curing conditions with the ACI 365 and ACI 318 regulations, this mixing design achieved the most closeness in the results. And also, in the results of compressive, tensile and flexural strengths for mixing design N and then design T-N80K20 (in concentrations of 8 M and 12 M and at curing temperatures

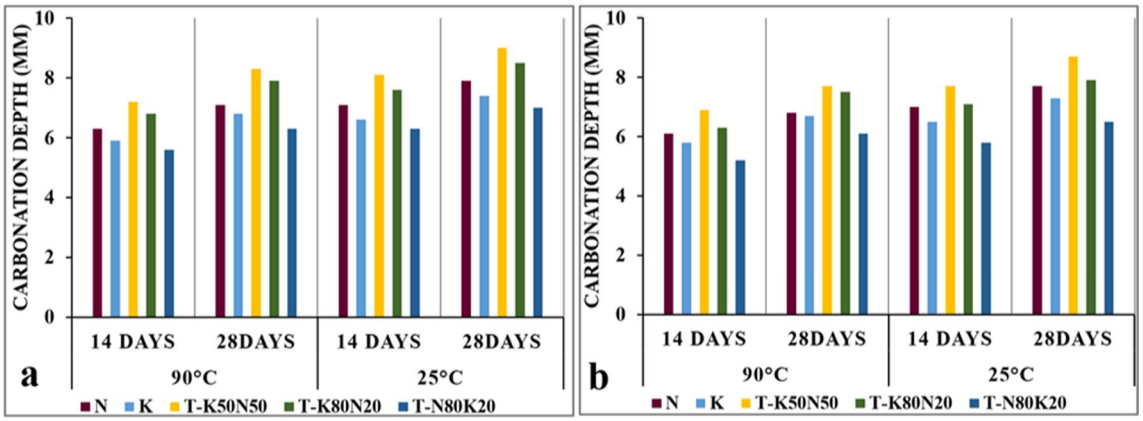

Fig. 23 Carbonation plot of samples **a**. 8 and **b**. 12 M cured at temperatures of 90 and 25 °C

Table 17 Carbonation test results from samples cured at 90 and 25 °C

Samples	25 °C	90 °C			Density (M)
	Carbonation depth at 14 days (mm)	Carbonation depth at 28 days (mm)	Carbonation depth at 14 days (mm)	Carbonation depth at 28 days (mm)	
K	7.1	7.9	6.3	7.1	8
N	6.7	7.4	6.1	6.6	
T-K50N50	8.1	9.0	7.2	8.1	
T-K80N20	7.9	8.5	6.8	7.6	
T-N80K20	6.3	7.0	5.6	6.3	
K	6.8	7.7	6.1	6.8	12
N	6.4	7.3	5.8	6.5	
T-K50N50	7.9	8.7	6.9	7.7	
T-K80N20	7.2	7.9	6.3	7.1	
T-N80K20	5.7	6.5	5.1	5.8	

of room and 90 degrees Celsius, a correlation relationship showed the best results.

According to the results obtained in this article, in the direction of sustainable development, it can be concluded that active alkaline concrete (geopolymer) in addition to environmental benefits has very good mechanical and durable properties; as a result, geopolymer concrete can be considered as a suitable alternative to conventional concrete (made of Portland cement) and environmentally friendly used in the construction industry.

Acknowledgements We hereby express our gratitude and appreciation for the support of Mr. Shahram Esparham and Babak Esparham.

Conflict of interest I declare that I have no conflicts of Interest in this work. My research is independent and not influenced by external factors such as financial resources, personal or professional relationships, or political affiliations. I have acted with integrity and honesty in doing so. By researching and analyzing the results, I have strictly adhered to the principles of academic integrity and ethical behavior throughout this project.

References

AC., Institute, AC. (1989). Building code requirements for reinforced concrete (ACI 318–89) and commentary--ACI 318R-89: American concrete institute.

Abdelmoamen M, Abdelsalam E (2020) Effect of potassium hydroxide and sodium silicate as an alkaline activator on the properties of GPC. Al-Azhar Uni Civ Eng Res Mag (CERM) 42(2):87–106

Ahmad S (1998) ACI-544, Measurement of properties of fiber reinforced concrete. Mater J 85:45–65

Aliabdo AA, Abd Elmoaty M, Emam MA (2019) Factors affecting the mechanical properties of alkali activated ground granulated blast furnace slag concrete. Constr Build Mater 197:339–355

Amran M, Al-Fakih A, Chu S, Fediuk R, Haruna S, Azevedo A, Vatin N (2021) Long-term durability properties of geopolymer concrete: an in-depth review. Case Stud Constr Mater 15:e00661

Bellum RR, Muniraj K, Madduru SRC (2020) Investigation on modulus of elasticity of fly ash-ground granulated blast furnace slag blended geopolymer concrete. Mater Today Proc 27:718–723

CA (2012). Standard test method for electrical indication of concrete's ability to resist chloride ion penetration. Paper presented at the american society for testing and materials.

Chau-Khun M, Zawawi AA, Wahid O (2018) Structural and material performance of geopolymer concrete. Constr Build Mater 186:90–102

Chen C, Zhang X, Hao H (2023) Investigation on the impact resistance of reinforced geopolymer concrete slab. J Clean Prod 406:137144. https://doi.org/10.1016/j.jclepro.2023.137144
Chindaprasirt P, Chalee W (2014) Effect of sodium hydroxide concentration on chloride penetration and steel corrosion of fly ash-based geopolymer concrete under marine site. Constr Build Mater 63:303–310
Commitee RCP (1984) RILEM draft recommendation: measurement of hardened concrete carbonation depth CPC-18. Mater Struct 17(102):435–440
Concrete, A. I. C. C. O., Aggregates, C (2017) Standard test method for splitting tensile strength of cylindrical concrete specimens1: ASTM international.
Concrete, F. I. B. I. F. S. (1990). High strength concrete joint FIP CEB state of the art report: FIB-international federation for structural concrete
Deepak AL, Lakshmi T (2020) Durability properties of geopolymer concrete with flyash and metakaolin. Int J Sci Technol Res 9:256–260
Dineshkumar M, Umarani C (2020) Effect of alkali activator on the standard consistency and setting times of fly ash and GGBS-based sustainable geopolymer pastes. Adv Civ Eng 2020:1–10
Elyamany HE, Abd Elmoaty M, Elshaboury AM (2018) Setting time and 7-day strength of geopolymer mortar with various binders. Constr Build Mater 187:974–983
EN, B. (2009). 12350–2. Testing fresh concrete. Slump-test. London: British standards institution.
Esparham A (2022a) A review of the features of geopolymer cementitious composites for use in green construction and sustainable urban development. Cent Asian J Environ Sci Technol Innov 3(3):64–74
Esparham A (2022b) Synthesis of environmentally friendly activated alkali concrete (geopolymer) Based on bentonite. J Environ Friendly Mater 6(2):1–8
Esparham A, Ghalatian F (2022) The features of geopolymer concrete as a novel approach for utilization in green urban structures. J Compos Compd 4(11):89–96
Esparham A, Moradikhou AB (2021a) Factors influencing compressive strength of fly ash-based geopolymer concrete. Amirkabir J Civ Eng 53(3):21–21
Esparham A, Moradikhou AB (2021b) A novel type of alkaline activator for geopolymer concrete based on class c fly ash. Adv Res Civ Eng 3(1):1–13. https://doi.org/10.30469/arce.2021.130143
Esparham A, Moradikhou AB (2021c) A novel type of alkaline activator for geopolymer concrete based on metakaolin. J Civ Eng Mater Appl 5(2):14–30
Esparham A, Moradikhou AB, Jamshidi Avanaki M (2020) Effect of various alkaline activator solutions on compressive strength of fly ash-based geopolymer concrete. J Civ Eng Mater Appl 4(2):115–123
Esparham A, Moradikhou AB, Mehrdadi N (2021) Introduction to synthesise method of Geopolymer concrete and corresponding properties. J Iran Ceram Soc 16(4):13–24
Esparham A, Vatin NI, Kharun M, Hematibahar M (2023) A study of modern eco-friendly composite (geopolymer) based on blast furnace slag compared to conventional concrete using the life cycle assessment approach. Infrastructures 8(3):58
Farooq F, Rahman SKU, Akbar A, Khushnood RA, Javed MF (2020) A comparative study on performance evaluation of hybrid GNPs/CNTs in conventional and self-compacting mortar. Alex Eng J 59(1):369–379
fur Normung, D. (1991). Testing concrete: Testing of Hardened concrete (Specimens prepared in mould) DIN 1048 Part 5 1991. In: Germany
Gunasekara C, Law DW, Setunge S (2016) Long term permeation properties of different fly ash geopolymer concretes. Constr Build Mater 124:352–362
Hardjito D, Rangan BV (2005) Development and properties of low-calcium fly ash-based geopolymer concrete. Research Report GC 1; Faculty of Engineering Curtin University of Technology: Perth, Australia
Hasanzadeh A, Vatin NI, Hematibahar M, Kharun M, Shooshpasha I (2022) Prediction of the mechanical properties of basalt fiber reinforced high-performance concrete using machine learning techniques. Materials 15(20):7165
Hassan A, Arif M, Shariq M (2022) Age-dependent compressive strength and elastic modulus of fly ash-based geopolymer concrete. Struct Concr 23(1):473–487
Huang Q, Tao Z, Pan Z, Wuhrer R, Rahme M (2022) Use of sodium/potassium citrate to enhance strength development in carbonate-activated hybrid cement. Constr Build Mater 350:128913
Jafari Nadoushan M, Ramezanianpor A (2019) Mechanical properties of alkali activated slag pastes and determination of optimum values of effective factors. Amirkabir J Civ Eng 50(6):1043–1052
Jan A, Pu Z, Khan KA, Ahmad I, Shaukat AJ, Hao Z, Khan I (2022) A review on the effect of silica to alumina ratio, alkaline solution to binder ratio, calcium oxide+ ferric oxide, molar concentration of sodium hydroxide and sodium silicate to sodium hydroxide ratio on the compressive strength of geopolymer concrete. SILICON 14(7):3147–3162
Jindal B, Singhal D, Sharma S, Jangra P (2018) Enhancing mechanical and durability properties of geopolymer concrete with mineral admixture. Comput Concr. https://doi.org/10.12989/cac.2018.21.3.000
Khan M, Castel A, Noushini A (2017) Carbonation of a low-calcium fly ash geopolymer concrete. Mag Concr Res 69(1):24–34
Kumar H, Prasad R, Srivastava A, Vashista M, Khan M (2018) Utilisation of industrial waste (fly ash) in synthesis of copper based surface composite through friction stir processing route for wear applications. J Clean Prod 196:460–468
Kushartomo W (2020) Mechanical properties of powder concrete with a geopolymer bond. Paper presented at the IOP conference series: materials science and engineering
Li W, Shumuye ED, Shiying T, Wang Z, Zerfu K (2022) Eco-friendly fibre reinforced geopolymer concrete: a critical review on the microstructure and long-term durability properties. Case Stud Constr Mater 16:e00894
Lim YY, Pham TM (2021) Influence of Portland cement on performance of fine rice husk ash geopolymer concrete: strength and permeability properties. Constr Build Mater 300:124321
Lokuge W, Wilson A, Gunasekara C, Law DW, Setunge S (2018) Design of fly ash geopolymer concrete mix proportions using multivariate adaptive regression spline model. Constr Build Mater 166:472–481
Meesala CR, Verma NK, Kumar S (2020) Critical review on fly-ash based geopolymer concrete. Struct Concr 21(3):1013–1028
Mehta A, Siddique R, Singh BP, Aggoun S, Łagód G, Barnat-Hunek D (2017) Influence of various parameters on strength and absorption properties of fly ash based geopolymer concrete designed by Taguchi method. Constr Build Mater 150:817–824
Mousavinejad SHG, Sammak M (2021) Strength and chloride ion penetration resistance of ultra-high-performance fiber reinforced geopolymer concrete. Elsevier, Structures, pp 1420–1427
Nath P, Sarker PK (2017) Flexural strength and elastic modulus of ambient-cured blended low-calcium fly ash geopolymer concrete. Constr Build Mater 130:22–31
Nguyen TT, Goodier CI, Austin SA (2020) Factors affecting the slump and strength development of geopolymer concrete. Constr Build Mater 261:119945

Nikvar-Hassani A, Manjarrez L, Zhang L (2022) Rheology, setting time, and compressive strength of class f fly ash-based geopolymer binder containing ordinary portland cement. J Mater Civ Eng 34(1):04021375

Noushini A, Castel A (2018) Performance-based criteria to assess the suitability of geopolymer concrete in marine environments using modified ASTM C1202 and ASTM C1556 methods. Mater Struct 51(6):146

Noushini A, Aslani F, Castel A, Gilbert RI, Uy B, Foster S (2016) Compressive stress-strain model for low-calcium fly ash-based geopolymer and heat-cured Portland cement concrete. Cement Concr Compos 73:136–146

Olivia M, Sarker P, Nikraz H (2008) Water penetrability of low calcium fly ash geopolymer concrete. Proc ICCBT2008-A 46:517–53046

Ouyang X, Shi C, Wu Z, Li K, Shan B, Shi J (2020) Experimental investigation and prediction of elastic modulus of ultra-high performance concrete (UHPC) based on its composition. Cem Concr Res 138:106241

Pasupathy K, Sanjayan J, Rajeev P (2021) Evaluation of alkalinity changes and carbonation of geopolymer concrete exposed to wetting and drying. J Build Eng 35:102029

Phoo-ngernkham T, Maegawa A, Mishima N, Hatanaka S, Chindaprasirt P (2015) Effects of sodium hydroxide and sodium silicate solutions on compressive and shear bond strengths of FA–GBFS geopolymer. Constr Build Mater 91:1–8

Quang Minh D, Bùi Thu H, Nguyen HT (2019) Effects of seawater content in alkaline activators to engineering properties of fly ash-based geopolymer concrete. Solid State Phenom 296:105–111. https://doi.org/10.4028/www.scientific.net/SSP.296.105

Rahman A, Majumder A (2013) Effects of missing value estimation methods in correlation matrix-a case study of concrete compressive strength data. Int J Adv Sci Technol 52(04):2013

Ranjbar N, Kuenzel C, Spangenberg J, Mehrali M (2020) Hardening evolution of geopolymers from setting to equilibrium: a review. Cement Concr Compos 114:103729

Rehman SKU, Imtiaz L, Aslam F, Khan MK, Haseeb M, Javed MF, Alabduljabbar H (2020) Experimental investigation of NaOH and KOH mixture in SCBA-based geopolymer cement composite. Materials 13(15):3437

Russell HG, Anderson AR, Banning JO, Cantor IG, Carrasquillo RL, Cook JE, Aitcin PC (1997) State-of-the-art report on high-strength concrete. ACI Committee 363:92

Saravanan S, Elavenil S (2018) Strength properties of geopolymer concrete using M sand by assessing their mechanical characteristics. ARPN J Eng Appl Sci 13(13):4028–4041

Shadnia R, Zhang L, Li P (2015) Experimental study of geopolymer mortar with incorporated PCM. Constr Build Mater 84:95–102

Shilar FA, Ganachari SV, Patil VB, Khan TY, Javed S, Baig RU (2022) Optimization of alkaline activator on the strength properties of geopolymer concrete. Polymers 14(12):2434

Sipos PM, Hefter G, May PM (2000) Viscosities and densities of highly concentrated aqueous MOH solutions (M+= Na+, K+, Li+, Cs+,(CH3) 4N+) at 2.50° C. J Chem Eng Data 45(4):613–617

Standard B (1983) 116 Testing concrete-method for determination of compressive strength of concrete cubes. British standards institute, London, United Kingdom

Standard A (2010) Standard test method for static modulus of elasticity and poisson's ratio of concrete in compression. ASTM Stand. C, 469

Tennakoon C, San Nicolas R, Sanjayan JG, Shayan A (2016) Thermal effects of activators on the setting time and rate of workability loss of geopolymers. Ceram Int 42(16):19257–19268

Testing A. S. F., Materials (2001a) ASTM C293, Standard test method for flexural strength of concrete (using simple beam with center-point loading)

Testing, A. S. F., Materials (2001b) ASTM C642: Standard test method for density, absorption, and voids in hardened concrete

Verma M, Dev N (2021) Sodium hydroxide effect on the mechanical properties of flyash-slag based geopolymer concrete. Struct Concr 22:E368–E379

Zhuguo L, Sha L (2018) Carbonation resistance of fly ash and blast furnace slag based geopolymer concrete. Constr Build Mater 163:668–680